Diffuseness effect and radial basis function network to optimize the calculation of α decay*

Na-Na MA(马娜娜)[1] Xiao-Jun BAO(包小军)[3] Hong-Fei ZHANG(张鸿飞)[1†]

[1]School of Nuclear Science and Technology, Lanzhou University, 730000 Lanzhou, China
[3]Department of Physics, Collaborative Innovation Center for Quantum Effects, and Key Laboratory of Low Dimensional Quantum Structures and Quantum Control of Ministry of Education, Hunan Normal University, Changsha 410081, People's Republic of China

Abstract: Radial basis function network (RBFN) approach is adopted for the first time to optimize the calculation of α decay half-life in the generalized liquid drop model (GLDM) concurrently incorporating the surface diffuseness effect. Calculations of the present study are in good agreement with the experimental half-lives for 68 superheavy nuclei (SHN), and a remarkable reduction of 40% in the root-mean-square (rms) deviations of half-lives is achieved. After that, based on RBFN method, the half-lives for four SHN isotopes, $^{252\text{-}288}$Rf, $^{272\text{-}310}$Fl, $^{286\text{-}316}$119 and $^{292\text{-}318}$120, are predicted using the improved GLDM with the diffuseness correction and the decay energies from WS4 and FRDM as inputs. Hence, we conclude that the diffuseness effect should be embodied in the proximity energy. Simultaneously, the neural network methods are encouraged to widely used in nuclear reaction.

Keywords: α decay, radial basis function network, the surface diffuseness effect

DOI:

I. INTRODUCTION

With the synthesis of superheavy nuclei (SHN) via the cold and hot fusion reactions in experiments [1-3], it is challenging to synthesize $Z \geqslant 118$ SHN and to explore the existence limit of SHN in nuclear physics[4-9]. Hence, the research of the stability and decay properties of the SHN is crucial [10-18]. As one of the dominant decay channels of the SHN, α decay provides an efficient approach to extract nuclear structure properties of the SHN, simultaneously, to identify new elements via the observation of α decay from an unknown parent nucleus to a known daughter one. To reproduce the experimental α decay half-life of the known SHN with a high accuracy and achieve a reliable extrapolation in the unknown SHN region, some physical effects and methods should be explored.

Theoretically, α decay is regarded as the progress of an α particle tunneling through the potential barrier between the α cluster and the daughter nucleus. The surface diffuseness as a main parameter in the proximity energy [19-36], is usually handled in the two cases (see Table 1): the fixed constant a_{eff} refers to the case with equal diffuseness parameters for all nuclei; the non-constant a_{eff} to the case with various diffuseness values for different nuclei. Recently, these non-constant surface diffuseness are adopted to achieve more accurate α decay calculations [32-36]. It is worth noting that Dehghani *et al*. investigated the best surface diffuseness values by matching the experimental half-life for SHN and found the diffuseness a_{eff} is in the range of $0.1-0.9$ fm [35]. Later Abdul-latif and Nagib derived a semiempirical formula of diffuseness in Ref. [36] and achieved a reliable extrapolation. These researches shown that the diffuseness of the nuclear surface, thus reflects in the the proximity energy in α decay, is enhancing in the SHN region and should be regarded as an important degree-of-freedom in the α decay calculations.

In addition, radial basis function network (RBFN) is an artificial neural network and has been used in many researches [37]. In the study of nuclear properties, radial basis function (RBF) combined with various nuclear mass models, such as marco-micro Weizsäcker-Skyrme mass models (WS) and the covariant density functional theory [38-44], have made remarkable improvements in the accuracy and prediction of nuclear mass. Especially, the RBF approach has been employed to analyze the sources of mass deviations and study the correlation between nuclear effective interactions and the distributions of mass deviation [45], which further gives a new way for improving the nuclear mass predictions towards 100 keV accuracy. Up to now a lot of α decay data for SHN was

Received 1 January 2020

* Supported by the National Natural Science Foundation of China(No. 11947229, No. 11675223 and No. 11675066), the China Postdoctoral Science Foundation (No. 2019M663853), the Fundamental Research Funds for the Central Universities Grant No. lzujbky-2017-ot04 and Feitian Scholar Project of Gansu province

† E-mail: zhanghongfei@lzu.edu.cn

Table 1. The fixed and various surface diffuseness in different models. $I_d = \frac{N_d - Z_d}{A_d}$ denotes the isospin asymmetry of daughter nucleus.

	fixed constant $a_{\rm eff}$ (fm)							non-constant parameter $a_{\rm eff}$ (fm)			
Ref.	[20]	[21-23]	[24]	[25]	[26]	[27, 28]	[29, 30]	[31]	[32, 33]	[34]	[36]
$a_{\rm eff}$	0.493	0.54	0.596	0.60	0.63	0.65	0.67	0.70(0.75)	$0.5+0.33I_d$	$1.03-2.09A_d^{\frac{1}{3}}$	$-1.095+0.012Z+0.002N$

detected in experiments. These experimental data form a two-dimensional plane about (Z,N). Coincidentally, the RBFN method is an image reconstruction technique based on the Fourier transform. Hence these available data can be used to train the RBFN approach in the α decay calculation. Then the RBFN method captures lots of information from the experimental data.

Inspired by the suggestion that the surface diffuseness should be an important degree-of-freedom in alpha-daughter nucleus interaction potential. In this work, to quantitatively analyze the diffuseness effect on α decay half-life, the diffuseness effect will be introduced into the generalized liquid drop model (GLDM). In addition, it is meaningful to check that the RBFN approach can optimize the calculation of α decay. Hence, in this paper, an expression of diffuseness and the RBFN approach are introduced in GLDM in Sec. **2**. Detailed investigations of the diffuseness effect and the RBFN method on α decay half-lives of 68 SHN are discussed. Furthermore, the surface diffuseness and RBFN corrections both work for the calculation of α decay for $^{272\text{-}310}$Fl, $^{286\text{-}316}$119 and $^{292\text{-}318}$120 SHN isotopes in Sec. **3**. Finally, some conclusions are drawn in Sec. **4**.

II. THE SURFACE DIFFUSENESS EFFECT AND THE RADIAL BASIC FUNCTION NETWORK

A. Diffuseness correction in GLDM

The generalized liquid drop model (GLDM) has been successfully employed to describe the nuclear decays [46-48]. The macroscopic energy of the deformed nucleus is $E(r) = E_V + E_S + E_C + E_{\rm prox}$ [49]. The proximity energy in GLDM is regarded as the additional surface effect and is the contribution due to the attractive nuclear forces when a neck or a gap between separated fragments appears [50]. The proximity energy reads [50]

$$E_{\rm prox} = 2\gamma \int_{h_{\rm min}}^{h_{\rm max}} \Phi\left[\frac{D(r,h)}{b}\right] 2\pi h dh. \tag{1}$$

Where γ is the geometric mean between the surface parameters of the α cluster and daughter nucleus, and can be characterized by the isospin asymmetry (I_α and I_d) of two fragments,

$$\gamma = 0.9517\sqrt{(1-2.6I_\alpha^2)(1-2.6I_d^2)}\ {\rm MeV/fm^2}. \tag{2}$$

h is the transverse distance varying in $\left(a, \min\left(\frac{c_1}{2\sqrt{1-s^2}}, \frac{c_2}{2\sqrt{1-s_2^2}}\right)\right)$. Φ denotes the proximity function and D is the distance between the opposite surfaces in consideration. The surface width $b = \frac{\pi}{\sqrt{3}}a_{\rm eff}$ in the proximity energy is fixed at 0.99 fm and is a dependency of the surface diffuseness $a_{\rm eff}$. Hence the diffuseness $a_{\rm eff}$ is a constant for all nuclei in the previous calculations, with a typical value of 0.54 fm.

Inspired by the effect of surface diffuseness on α decay calculations, we introduce the diffuseness effect in GLDM and systematically investigate this effect in the calculation of α decay. The diffuseness of SHN has been explored to be correlated with the proton, neutron and mass number, or the isospin asymmetry I_d (see Table 1). We posit the ansatz that $a_{\rm eff}$ is a function of the effective sharp radius, i.e. $R_0 = 1.28A^{1/3} - 0.76 + 0.8A^{-1/3}$ [51], which is also proportional to the mass number. Hence it not only bridges up the relationship between the mass number and the surface diffuseness, but also reduces the introduction of additional parameters. In addition, the results of Ref. [35] shown that most values of $a_{\rm eff}$ for odd-X ($X = Z, N$ and A) nuclei are smaller than 0.54 fm. Simultaneously, these odd-X nuclei live longer than the even-Z and even-N ones around them [52]. Here, these differences depending on odd-even property of nuclei is considered in this calculation. After a fitting procedure, an expression of surface diffuseness in GLDM is obtained,

$$a_{\rm eff} = 0.075R_0 - 0.15({\rm mod}(Z,2) + {\rm mod}(N,2)), \tag{3}$$

for even-X nuclei, ${\rm mod}(X,2) = 0$; odd-X nuclei, ${\rm mod}\,(X,2) = 1$.

In the GLDM, the α decay half-life can be obtained by

$$T = \ln 2\lambda, \qquad \lambda = P_\alpha \nu_0 P_0. \tag{4}$$

Here, $\nu_0 = \frac{1}{2R}\sqrt{(2E_\alpha)/M_\alpha}$ denotes the assault frequency in Ref. [53]. The preformation factor P_α is adopted by an analytic formula, $P_\alpha = \exp[a + b(Z-Z_1)(Z_2-Z) + c(N-N_1)(N_2-N) + dA]$. The penetration probability P_0 is calculated within the WKB approximation,

$$P_0 = \exp\left\{-\frac{2}{\hbar}\int_{R_{\rm in}}^{R_{\rm out}} \sqrt{2\mu[E(r) - Q_\alpha]}dr\right\}, \tag{5}$$

where μ denotes the reduced mass, $R_{\rm in} = R_\alpha + R_d$ and $R_{\rm out} = e^2 Z_\alpha Z_d / Q_\alpha$ are the two turning points of the WKB action integral, where R_α and R_d are the radius of two fragments.

B. The Radial Basis Function Network (RBFN) method

The general architecture of the RBFN method in the calculation of α decay is shown in Fig. 1. The RBFN approach uses radial basis functions as activation functions and the corresponding form is [38-40, 42, 43]

$$S(x) = \sum_{i=1}^{m} \omega_i \phi(\|x - x_i\|), \tag{6}$$

here $S(x)$ is the reconstructed smooth function, $\phi(r)$ the radial basis function. The output of the network is a linear combination of radial basis functions of the inputs and neuron parameters. m the number of data points to be fitted, x_i the point from measurement. ω_i denotes the weight of the center x_i and is obtained by solving the matrix equation of $\phi(r)$ and the deviation between the experimental half-life and the calculated data. Inserting ω_i into Eq. (6), one can get the corresponding smooth function $S(x_i)$.

With the help of the global interpolation and extrapolation of the RBFN method, one can predict the α decay half-life of an unmeasured nucleus by using the experimental data. In other words, the half-life predictions for unmeasured nuclei can be treated as a problem of half-life surface extrapolation from the experimental data.

Nuclei taken into account in our calculations and the corresponding experimental data are from Ref. [36] are shown in Fig. 2(a), where $104 \leqslant Z \leqslant 118$. To improve the accuracy of half-life more effectively, 68 SHN are divided into four categories: even Z-even N, even Z-odd N, odd Z-even N, odd Z-odd N. After considering the RBFN approach, the revised logarithm of α decay half-life is

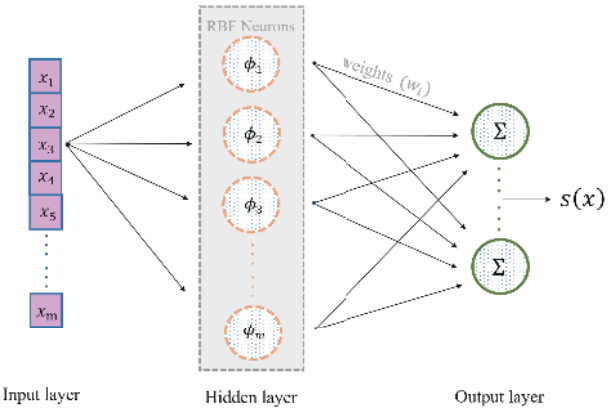

Fig. 1. (Color online) The architecture of the RBFN approach in α decay calculation.

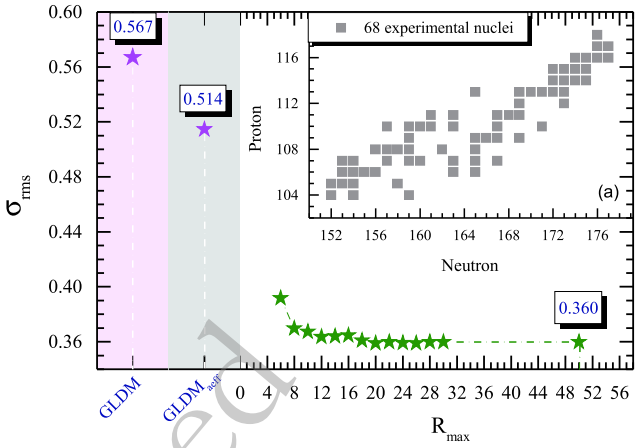

Fig. 2. (Color online) Distributions of 68 superheavy nuclei (a); Magenta stars denote the rms deviations of half-life from GLDM with/without the surface diffuseness effect. Olive stars describe the convergent behavior of the rms deviations in RBFN approach.

$$\mathrm{Log}_{10} T^{\rm RBFN}_{\rm aeff}(Z,N) = \mathrm{Log}_{10} T_{\rm aeff}(Z,N) + S(Z,N). \tag{7}$$

Here, $\mathrm{Log}_{10} T_{\rm aeff}(Z,N)$ denotes the result of the GLDM incorporating the diffuseness effect.

III. RESULTS AND DISCUSSION

A. Calculation of α decay for the known SHN

There are several forms of the Euclidean norm $\phi(r)$ in the RBFN approach, such as Gaussian, $\phi(r) = \exp^{-(\varepsilon r)^2}$; multiquadric, $\phi(r) = 1 + (\varepsilon r)^2$; inverse quadric, $\phi(r) = \sqrt{1 + (\varepsilon r)^2}$, and so on. We test the possible form of $\phi(r)$ and find an interesting phenomenon that $\phi(r) = r$, i.e. $\|x - x_i\| = \sqrt{(Z_i - Z_j)^2 + (N_i - N_j)^2}$, which stands for the distance between nucleus (Z_i, N_i) and (Z_j, N_j), gives better theoretical half-life than the aforementioned forms. This form is also suitable for the study of nuclear mass.

The root-mean-square (rms) deviations with respect to the half-lives $(\sigma_{\rm rms})^2 = \frac{1}{n}\sum_{i=1}^{n} |\mathrm{Log}_{10} T^{\rm Exp}_{1/2} - \mathrm{Log}_{10} T^{\rm Cal}_{1/2}|^2$ is introduced to evaluate quantitative precision of the theoretical calculations. The value of $\sigma_{\rm rms}$ under the GLDM with $a_{\rm eff}$ fixed at 0.54 fm is 0.567. By introducing the semiempirical formula of diffuseness [see Eq. (3)] into the GLDM, the rms deviations of half-life is reduced from 0.567 to 0.514 by up to 10%. Also, one need to test the convergent behavior of the RBFN method. It is worth pointing out that the r is in the range of $R_{\rm min} \leqslant r \leqslant R_{\rm max}$. In Fig. 2, when $R_{\rm max} = 0$, the reconstructed function $S(Z,N)$ is zero. Thus, $\mathrm{Log}_{10} T^{\rm RBFN}_{\rm aeff}(Z,N) = \mathrm{Log}_{10} T_{\rm aeff}(Z,N)$, which means without the RBFN approach. Because there are 68 nuclei we used (see Fig. 2(a)) and some nuclei are relatively scattered, thus the effective value of $R_{\rm min} = 6$ in this work. One can see that the accuracy of prediction

reaches to a convergence at $R_{\max} > 20$ for 68 SHN. The value of $\sigma_{\rm rms}$ is reduced from 0.514 to 0.360, a total reduction of 40%. Noted that the calculated half-lives of most odd-X nuclei are worse than these of even Z-even N nuclei in GLDM, and the weight depends on the deviation in RBFN approach. Hence, the value of $\sigma_{\rm rms}$ is only 0.538 under GLDM+RBFN without considering the surface diffuseness effect. While the introduction of the surface diffuseness effect in GLDM makes the description of most odd-X nuclei better in $\rm GLDM_{aeff}$. Thus, RBFN method will capture this effective information and optimize those nuclei with large deviations, which in turn makes the results of RBFN better.

To figure out how the effect of odd-even property on surface diffuseness parameter and RBFN approach, the rms deviations for these four categories: even Z-even N, even Z-odd N, odd Z-even N, odd Z-odd N, are listed in Table 2. After the surface diffuseness effect is included into the proximity energy in GLDM, the $\sigma_{\rm rms}$ value reduces to a certain extent. Unfortunately, there still exists a slight systematic difference for the congeneric nuclei of even Z-odd N. This is because we perform the fitting scheme for 68 SHN at the same time, the sigma values for four groups, e-e, e-o, o-e and o-o nuclei, are the results of overall systematics. Thus some nuclei with large deviations between the experimental half-lives and the theoretical ones, such as ^{267}Ds, leads to the sigma value of e-o nuclei is larger than the results of GLDM without diffuseness effect. In addition, since GLDM is semi-classical theoretical model and the blocking effect of unpaired nucleons is not introduced into. Also, the sigma value is affected by the experimental half-life to a certain extent in SHN region. One can find that all models (GLDM, $\rm GLDM_{aeff}$, and $\rm GLDM_{aeff}^{RBF}$) can better describe the alpha decay half-lives of o-e than e-o nuclei. While with the implementation of the RBFN approach, the obtained rms deviations for four categories are about 16%-50% less than before, which indicates a very significant improvement for half-life calculations.

The $a_{\rm eff}$ values, the contributions of RBFN approach for the 68 SHN are tabulated in Table 3. The corresponding deviations between the experimental half-life and the theoretical data, the Gaussian statistical behaviors (denoted by blues dash line) are respectively shown in the top and bottom panels in Fig. 3. One can find that a reduction of $a_{\rm eff}$ around 0.1 fm can increase the value of $\rm Log_{10}T_{\frac{1}{2}}$ by 0.1 s. The values of $a_{\rm eff}$ (seventh and fifteenth columns) have a good match with the diffuseness values in Ref. [35] (Table 1) and Ref. [36] (Table 1). Three sets of $a_{\rm eff}$ indicate that the diffuseness values of odd-Z or (and) odd-N nuclei are less than 0.54 fm. This indicates that including odd-even effect in surface diffuseness parameter, to some extent, is equivalent to the introduction of the blocking effect of unpaired nucleons in GLDM. Note that the calculated half-lives of GLDM

Table 2. Comparison of the rms deviations for these four categories: even Z-even N, even Z-odd N, odd Z-even N, odd Z-odd N, under GLDM, GLDM with diffuseness effect in Eq. (3) (labeled as $\rm GLDM_{aeff}$) and GLDM incorporating both diffuseness effect and RBFN approach (tagged $\rm GLDM_{aeff}^{RBFN}$), respectively.

Models	$\sigma_{\rm rms}$			
	e-e	e-o	o-e	o-o
GLDM	0.272	0.510	0.350	0.794
$\rm GLDM_{aeff}$	0.233	0.576	0.278	0.656
$\rm GLDM_{aeff}^{RBFN}$	0.201	0.421	0.270	0.412

with the fixed $a_{\rm eff}$ = 0.54 fm in SHN region are systematically higher than these of *prox* model and the *universal decay law* (UDL) in Ref. [54]. By incorporating diffuseness effect, the changes of surface behavior of nucleus optimize the proximity energy thus the potential barrier of reaction system, hence improving the half-life calculation. It is worth pointing out that the semiempirical formula of diffuseness [the Eq. (15) in Ref. [36]] proposed by Nagib *et al.* indeed improve the calculation of half-life, even though this expression does not work well in GLDM framework. Together with the results shown in Fig. 3, we find the surface diffuseness effect optimizes the calculation comparing the results by the conventional model, especially for these nuclei whose calculated half-lives in GLDM were always higher than the experimental data. Then the corresponding deviations between the experimental half-life and the theoretical data in $\rm GLDM_{aeff}$ show a good Gaussian distribution.

In addition, the RBFN approach introduces a remarkable improvement on the half-life, these differences are almost populated between 1 and -1 and systematically smaller than these from the GLDM with/without surface diffuseness effect, as shown in Fig. 3. The corresponding reconstructed functions $S(Z,N)$ are shown in Table 3. One can find an inseparable connection exists between the $S(Z,N)$ of the RBFN correction and the deviations between the experimental half-life and the theoretical data in $\rm GLDM_{aeff}$. As the weight ω_i determines the value of the reconstructed function $S(x_i)$ according to the deviation, the relatively large deviations between theoretical calculations and experimental data can be compensated by the RBFN approach. Especially for these nuclei, ^{260}Bh, ^{265}Hs, ^{268,274}Mt, ^{272,274}Rg, ^{278}Nh and ^{291,293}Lv. Take ^{260}Bh as an example, the $\rm Log_{10}T_{\frac{1}{2}}$ is changed from -2.543 s in the conventional GLDM to -1.26 s with both the diffuseness and RBFN corrections, which has been increased by more than 50%. More interesting, we find that such reduced deviation is not a monotonic improvement. Most of the theoretical half-lives are getting closer to the corresponding experimental values, no matter the theoretical value is larger or smaller than the experimental value.

Table 3. The calculations for the 68 SHN. The first column is the element. The corresponding experimental $Q_\alpha^{\rm Exp}$, the logarithm of half-lives from experiments, GLDM, $\rm GLDM_{aeff}$ and $\rm GLDM_{aeff}^{RBFN}$, the $a_{\rm eff}$ and S values in order. The right half of the Table same as the left half.

Nuclei	$Q_\alpha^{\rm Exp}$ (MeV)	$\rm Log_{10}T_{\frac{1}{2}}$ (s)				$a_{\rm eff}$ (fm)	S (s)	Nuclei	$Q_\alpha^{\rm Exp}$ (MeV)	$\rm Log_{10}T_{\frac{1}{2}}$ (s)				$a_{\rm eff}$ (fm)	S (s)
		Exp	GLDM	$\rm GLDM_{aeff}$	$\rm GLDM_{aeff}^{RBFN}$					Exp	GLDM	$\rm GLDM_{aeff}$	$\rm GLDM_{aeff}^{RBFN}$		
$Z=104$								^{270}Ds	11.120	−4.000	−3.656	−3.735	−3.912	0.573	−0.177
^{256}Rf	8.926	0.319	0.227	0.165	0.079	0.562	−0.086	^{271}Ds	10.899	−2.639	−2.452	−2.333	−2.506	0.424	−0.173
^{258}Rf	9.190	−1.035	−0.686	−0.748	−0.707	0.564	0.041	^{273}Ds	11.380	−3.770	−3.718	−3.605	−3.784	0.425	−0.179
^{263}Rf	8.250	3.301	2.953	3.074	2.955	0.417	−0.119	^{277}Ds	10.720	−2.222	−2.393	−2.283	−2.133	0.428	0.151
$Z=105$								^{281}Ds	9.320	2.125	1.292	1.389	1.137	0.431	−0.252
^{257}Db	9.206	0.389	0.696	0.635	0.826	0.413	0.191	$Z=111$							
^{258}Db	9.500	0.776	−0.570	−0.307	0.437	0.264	0.744	^{272}Rg	11.197	−2.420	−3.494	−3.382	−1.976	0.274	1.406
^{259}Db	9.620	−0.292	−0.629	−0.502	−0.513	0.414	−0.011	^{274}Rg	11.480	−2.194	−4.147	−3.894	−3.048	0.276	0.846
^{263}Db	8.830	1.798	1.498	1.621	1.823	0.417	0.202	^{278}Rg	10.850	−2.377	−2.603	−2.349	−1.661	0.279	0.688
$Z=106$								^{279}Rg	10.530	−1.046	−1.581	−1.473	−1.431	0.429	0.042
^{259}Sg	9.804	−0.492	−0.692	−0.426	−0.934	0.414	−0.508	^{280}Rg	9.910	0.663	−0.071	0.156	0.267	0.280	0.111
^{260}Sg	9.901	−1.686	−1.878	−1.944	−2.056	0.565	−0.112	$Z=112$							
^{261}Sg	9.714	−0.638	−0.550	−0.424	−0.714	0.416	−0.290	^{281}Cn	10.460	−1.000	−1.087	−0.855	−0.855	0.431	0.000
^{262}Sg	9.600	−1.504	−1.128	−1.196	−1.228	0.567	−0.032	^{285}Cn	9.320	1.447	1.977	2.072	2.003	0.434	−0.069
^{269}Sg	8.700	2.079	2.075	2.188	2.253	0.422	0.065	$Z=113$							
^{271}Sg	8.670	2.219	2.070	2.182	2.356	0.424	0.174	^{278}Nh	11.850	−3.620	−4.513	−4.401	−3.420	0.279	0.981
$Z=107$								^{282}Nh	10.780	−1.155	−1.978	−1.742	−1.525	0.282	0.217
^{260}Bh	10.400	−1.459	−2.543	−2.414	−1.260	0.265	1.154	^{283}Nh	10.480	−1.000	−0.832	−0.733	−0.587	0.432	0.146
^{261}Bh	10.500	−1.899	−2.181	−2.051	−2.016	0.416	0.035	^{284}Nh	10.120	−0.041	−0.188	0.045	0.283	0.283	0.238
^{264}Bh	9.960	−0.357	−1.324	−1.048	−0.701	0.268	0.347	^{285}Nh	10.010	0.623	0.363	0.460	0.171	0.434	−0.289
^{266}Bh	9.430	0.230	0.206	0.457	1.080	0.270	0.623	^{286}Nh	9.790	0.978	0.808	1.042	0.900	0.285	−0.143
^{267}Bh	9.230	1.230	0.970	1.085	1.295	0.420	0.210	$Z=114$							
^{270}Bh	9.060	1.785	1.420	1.674	1.952	0.273	0.278	^{286}Fl	10.350	−0.699	−0.771	−0.674	−0.734	0.585	−0.060
^{272}Bh	9.310	1.000	0.687	0.923	0.995	0.274	0.072	^{287}Fl	10.170	−0.319	0.250	0.346	−0.264	0.435	−0.610
^{274}Bh	8.930	1.732	1.865	2.102	2.152	0.276	0.050	^{288}Fl	10.072	−0.180	−0.092	−0.179	−0.344	0.586	−0.165
$Z=108$								^{289}Fl	9.980	0.279	0.672	0.760	0.079	0.437	−0.681
^{264}Hs	10.591	−2.796	−2.973	−2.844	−2.869	0.568	−0.025	$Z=115$							
^{265}Hs	10.470	−2.699	−1.928	−1.808	−2.581	0.419	−0.773	^{287}Mc	10.760	−1.432	−0.915	−1.008	−1.209	0.435	−0.201
^{266}Hs	10.346	−2.638	−2.463	−2.534	−2.746	0.570	−0.212	^{288}Mc	10.630	−1.060	−1.108	−0.889	−0.818	0.286	0.071
^{267}Hs	10.037	−1.187	−0.906	−0.788	−1.151	0.420	−0.363	^{289}Mc	10.520	−0.658	−0.406	−0.316	−0.544	0.437	−0.228
^{270}Hs	9.050	0.556	1.084	1.010	0.715	0.573	−0.295	^{290}Mc	10.410	−0.187	−0.482	−0.261	−0.465	0.287	−0.204
^{273}Hs	9.730	−0.119	−0.410	−0.302	−0.293	0.425	0.009	$Z=116$							
$Z=109$								^{290}Lv	10.990	−1.824	−1.776	−1.686	−1.802	0.587	−0.116
^{268}Mt	10.670	−1.678	−2.704	−2.584	−2.146	0.271	0.438	^{291}Lv	10.890	−1.721	−1.064	−0.974	−1.683	0.438	−0.709
^{274}Mt	10.200	−0.357	−1.409	−1.164	−0.658	0.276	0.506	^{292}Lv	10.774	−1.745	−1.321	−1.415	−1.533	0.589	−0.118
^{275}Mt	10.480	−1.699	−2.107	−1.997	−1.631	0.427	0.366	^{293}Lv	10.680	−1.276	−0.621	−0.532	−1.223	0.440	−0.691
^{276}Mt	10.030	−0.347	−0.907	−0.660	−0.559	0.277	0.101	$Z=117$							
^{278}Mt	9.580	0.653	0.418	0.664	0.754	0.279	0.090	^{293}Ts	11.180	−1.854	−1.471	−1.567	−2.015	0.440	−0.448
$Z=110$								^{294}Ts	11.070	−1.745	−1.764	−1.535	−1.368	0.290	0.167
^{267}Ds	11.780	−5.553	−4.191	−3.922	−4.458	0.420	−0.536	$Z=118$							
^{269}Ds	11.509	−3.747	−3.724	−3.601	−4.495	0.422	−0.894	^{294}Og	11.820	−3.161	−3.109	−3.018	−3.309	0.590	−0.291

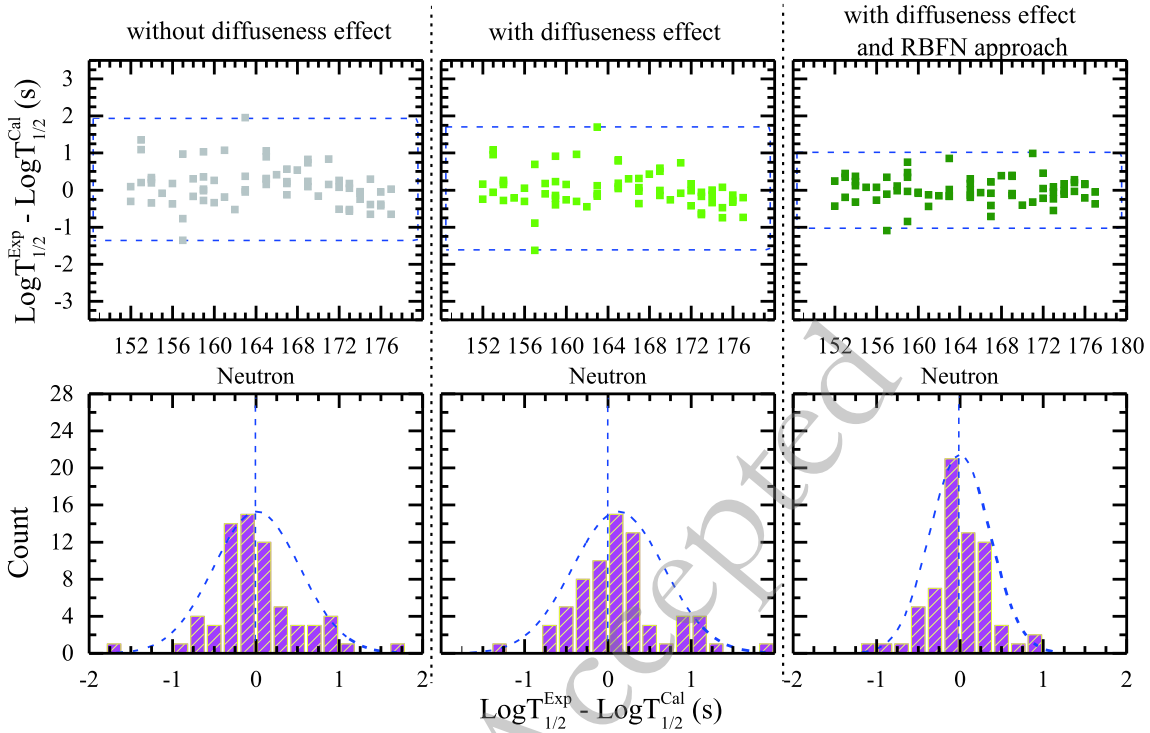

Fig. 3. (Color online) Differences between the experimental α decay half-life and the calculated one for 68 SHN in the top panel. Histgrams of these differences for GLDM, $GLDM_{aeff}$ and $GLDM_{aeff}^{RBFN}$ in the bottom panel. The corresponding Gaussian distributions are also shown with blue lines.

The result reveals that surface diffuseness effect play an important role in theoretical describing α decay. RBFN approach is a powerful tool to optimize the decay calculations.

B. Predictions of α decay properties of the SHN isotopes

Several theoretical works suggested the possible doubly magic nuclei beyond ^{280}Pb: ^{298}Fl in macroscopic-microscopic approach [55], ^{304}120 the relativistic Hartree-Fock-Bogoliubov (RHFB) theory [56], $Z = 124$, 126 and $N = 184$ the nonrelativistic Skyrme-Hartree-Fock models, and so on. In addition, with the synthesis of ^{294}Og SHN, ones attempt to produce the nuclei with $Z = 119$ and 120 [5-11, 15]. α decay is one of main decay modes of the SHN. Encouraged by the above improvements from RBFN approach and surface diffuseness effect, we predict the half-lives of four isotopes, $^{252\text{-}288}$Rf, $^{272\text{-}310}$Fl, $^{286\text{-}316}$119 and $^{292\text{-}318}$120. It is well known that the half-life is extremely sensitive to the decay energy and the barrier potential. Fig. 4 shows the variation of decay energy and the calculated half-life along different isotopic chains. Here, the decay energy Q_α^{WS4} (denoted by blue square) from the WS4 model [57] and Q_α^{FRDM} values (red circle) with FRDM model [58] as inputs.

On the one hand, the Q_α value and the corresponding $\mathrm{Log}_{10}T_{\frac{1}{2}}$ data show opposite trend while symmetrically, especially for $^{252\text{-}288}$Rf isotope. This is consistent with the Geiger-Nuttall law, $\mathrm{Log}_{10}T_{\frac{1}{2}} = a\frac{1}{\sqrt{Q_\alpha}} + b$. It is well known that half-life is extremely sensitive to the Q_α value. When Q_α has a large discrepancy between WS4 and FRDM, a similar behavior in half-lives also appears. For instance, a deviation of 1 MeV between Q_α^{WS4} and Q_α^{FRDM} leads to a difference of $\mathrm{Log}_{10}T_{\frac{1}{2}}$ ranging about 10^4 times for ^{282}Fl nucleus. On the other hand, the calculated α decay half-live improved by surface diffuseness effect and RBFN approach both increase with increasing neutron number up to a possible neutron magic number, then decrease with up to the possible neutron magic (or submagic) number plus two. After that, they increase again. It is well known that the shell effects for α radioactivity are related to the Q_α, which reaches to the maximum when the daughter nuclei has a magic number of neutrons and protons. Hence the trend of the two sets of decay energy, Q_α^{WS4} and Q_α^{FRDM}, is opposite to the half-life. Both the decay energy and half-life reflect the strong shell effects at $N = 184$, which confirms that the next neutron magic number after $N = 126$ is $N = 184$. Furthermore, $N = 152$, 162 and 178 are the possible candidates for neutron submagic numbers. It also shows that $N = 196$ is a possible neutron submagic number from the WS4 Q_α decay energy and the corresponding half-life of $Z = 119$ and 120 isotopes. In addition, the values of Q_α and

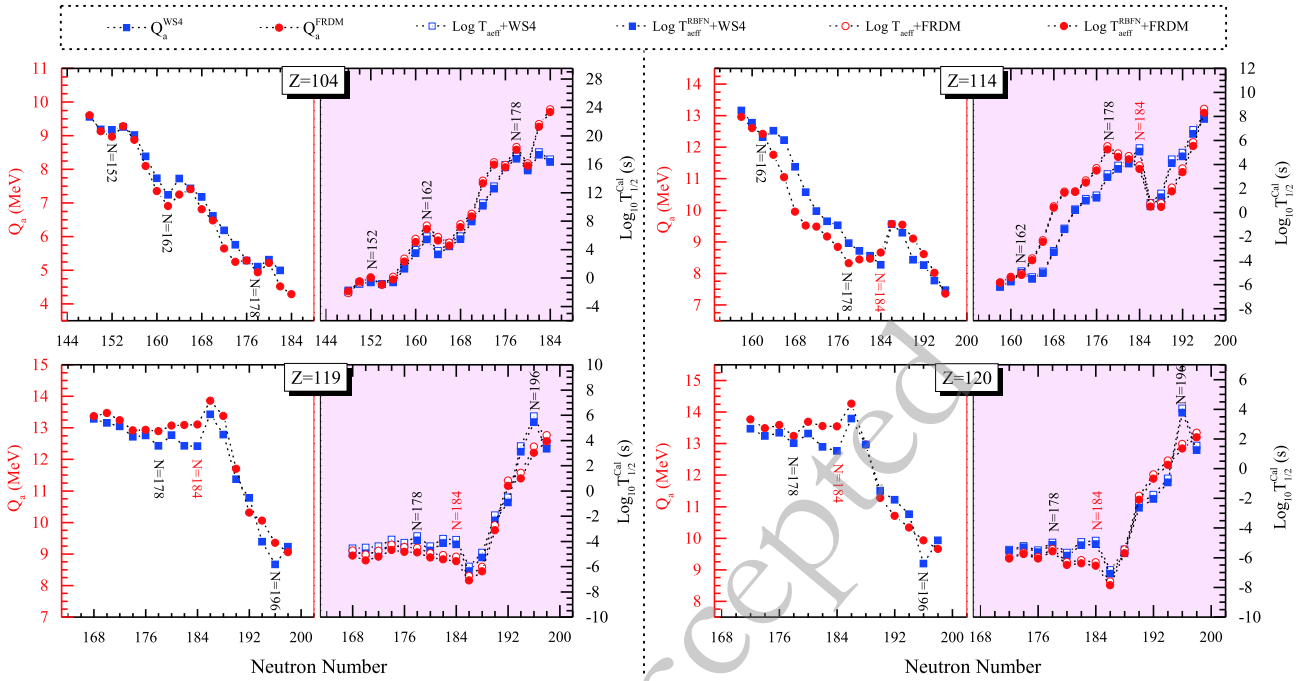

Fig. 4. The α decay energy Q_α respectively from WS4 [57] and FRDM [58] are denoted by blue square and red circle in the left side of subfigure. α decay half-life under $\mathrm{GLDM_{aeff}}$ and $\mathrm{GLDM_{aeff}^{RBFN}}$ for $Z=104,114,119$ and 120 isotopes (only even-N number are shown here) in the right side of subfigure.

$\mathrm{Log}_{10}T_{\frac{1}{2}}$ do not change too much between $N=178$ to 184. This indicates that nuclei in this region are relatively stable.

IV. SUMMARY

In summary, we introduce the surface diffuseness effect in the proximity energy via constructing an expression of diffuseness which depends on the effect sharp radius and an odd-even correction to improve the calculation of α decay. Meanwhile, the RBFN method is adopted to the α decay calculation for the first time. The rms deviations of 68 SHN in the GLDM framework are dropped from 0.567 to 0.360 by up to 40%. After that, we extrapolate the half-lives of $^{252\text{-}288}$Rf, $^{272\text{-}310}$Fl, $^{286\text{-}316}$119 and $^{292\text{-}318}$120 isotopes with WS4 and FRDM Q_α values as inputs. Two points can be summarized:

(i) The calculated α decay half-life reproduce the experimental data with a high accuracy by considering the RBFN method under the improved GLDM with diffuseness effect. Hence we conclude that the diffuseness effect as an important physical effect should be introduced into the calculation of α decay and spontaneous fission. The RBFN method is encouraged to be widely used in the study of nuclear reactions.

(ii) Both the decay energy and half-life of $^{252\text{-}288}$Rf, $^{272\text{-}310}$Fl, $^{286\text{-}316}$119 and $^{292\text{-}318}$120 isotopes indicate that $N=184$ is the candidate of neutron magic number and $N=152,162,178$ are neutron submagic numbers. $N=196$ is a possible neutron submagic number from the WS4 Q_α decay energy and the corresponding half-life.

References

[1] S. Hofmann, Rep. Prog. Phys. **61**, 639 (1998)
[2] S. Hofmann and G. Münzenberg, Rev. Mod. Phys. **72**, 733 (2000)
[3] Yu. Oganessian, J. Phys. G: Nucl. Part. Phys. **34**, R165 (2007)
[4] X. J. Bao, Y. Gao, J. Q. Li, and H. F. Zhang, Phys. Rev. C **91**, 011603(R) (2015)
[5] F. Li, L. Zhu, Z. -H. Wu, X. -B. Yu, J. Su, and C. -C. Guo, Phys. Rev. C **98**, 014618 (2018)
[6] L. Zhu, W. -J. Xie, and F. -S. Zhang, Phys. Rev. C **89**, 024615 (2014)
[7] K. P. Santhosh and V. Safoora, Phys. Rev. C **96**, 034610 (2017)
[8] N. Wang, E. -G. Zhao, W. Scheid, and S. -G. Zhou, Phys. Rev. C **85**, 041601(R) (2012)
[9] K. Siwek-Wilczyńska, T. Cap, M. Kowal, A. Sobiczewski, and J. Wilczyński, Phys. Rev. C **86**, 014611 (2012)
[10] Z. -H. Liu and J. -D. Bao, Phys. Rev. C **84**, 031602(R) (2011)
[11] Y. Z. Wang, S. J. Wang, Z. Y. Hou, and J. Z. Gu, Phys. Rev. C **92**, 064301 (2015)
[12] D. N. Poenaru and R. A. Gherghescu, Phys. Rev. C **97**, 044621 (2018)
[13] P. R. Chowdhury, C. Samanta, and D. N. Basu, Phys. Rev.

C **73**, 014612 (2006)
[14] Z. Ge, C. Li, J. Li, G. Zhang, B. Li, X. Xu, C. A. T. Sokhna, X. Bao, H. Zhang, Yu. S. Tsyganov, and F. -S. Zhang, Phys. Rev. C **98**, 034312 (2018)
[15] T. L. Zhao and X. J. Bao, Phys. Rev. C **98**, 064307 (2018)
[16] G. G. Adamian, N. V. Antonenko, H. Lenske, and L. A. Malov, Phys. Rev. C **101**, 034301 (2020)
[17] S. Q. Guo, X. J. Bao, H. F. Zhang, J. Q. Li, and N. Wang, Phys. Rev. C **100**, 054616 (2019)
[18] H. F. Zhang, Y. Gao, N. Wang, J. Q. Li, E. G. Zhao, G. Royer, Phys. Rev. C **85**, 014325 (2012)
[19] J. -G. Deng, H. -F. Zhang, and G. Royer, Phys. Rev. C **101**, 034307 (2020)
[20] J. -G. Deng, X. -H. Li, J. -L. Chen, J. -H. Cheng, and X. -J. Wu, Eur. Phys. J. A **55**, 58 (2019)
[21] V. Yu. Denisov and H. Ikezoe, Phys. Rev. C **72**, 064613 (2005)
[22] C. Xu and Z. Ren, Nucl. Phys. A **760**, 303 (2005); Phys. Rev. C **74**, 014304 (2006).
[23] C. Samanta, P. R. Chowdhury and D. N. Basu, Nucl. Phys. A **789**, 142 (2007)
[24] M. Ismail, W. M. Seif, A. Adel and A. Abdurrahman, Nucl. Phys. A **958**, 202 (2017)
[25] X. D. Sun, J. G. Deng, D. Xiang, P. Guo and X. H. Li, Phys. Rev. C **95**, 044303 (2017)
[26] D. Ni and Z. Ren, Nucl. Phys. A **825**, 145 (2009)
[27] Y. Qian, Z. Ren and D. Ni, Phys. Rev. C **83**, 044317 (2011)
[28] S. Dahmardeh, S. A. Alavi and V. Dehghani, Nucl. Phys. A **963**, 68 (2017)
[29] B. Buck, A. C. Merchant and S. M. Perez, Phys. Rev. C **51**, 559 (1995)
[30] S. B. Duarte, N. Teruya, Phys. Rev. C **85**, 017601 (2012)
[31] L. L. Li, S. G. Zhou, E. G. Zhao and W. Scheid, Int. J. Mod. Phys. E **19**, 359 (2010)
[32] H. Hassanabadi, E. Javadimanesh and S. Zarrinkamar, Nucl. Phys. A **906**, 84 (2013)
[33] R. I. Betan and W. Nazarewicz, Phys. Rev. C **86**, 034338 (2012)
[34] D. Ni and Z. Ren, Phys. Rev. C **81**, 064318 (2010)
[35] M. R. Pahlavani, S. A. Alavi and N. Tahanipour, Mod. Phys. Lett. A **28**, 1350065 (2013)
[36] V. Yu. Denisov, O. I. Davidovskaya and I. Yu. Sedykh, Phys. Rev. C **92**, 014602 (2015)
[37] V. Dehghani, S. A. Alavi, and Kh. Benam, Mod. Phys. Lett. A **33**, 1850080 (2018)
[38] A. Abdul-latif and O. Nagib, Phys. Rev. C **100**, 024601 (2019)
[39] M. D. Buhmann, *Radial Basis Functions: Theory and Imple-mentations* (Cambridge University Press, Cambridge, UK, 2003).
[40] N. Wang and M. Liu, Phys. Rev. C **84**, 051303(R) (2011)
[41] N. N. Ma, H. F. Zhang, X. J. Bao, P. H. Chen, J. M. Dong, J. Q. Li, and H. F. Zhang, J. Phys. G: Nucl. Part. Phys. **42**, 095107 (2015)
[42] Z. M. Niu, Z. L. Zhu, Y. F. Niu, B. H. Sun, T. H. Heng, and J. Y. Guo, Phys. Rev. C **88**, 024325 (2013)
[43] J. S. Zheng, N. Y. Wang, Z. Y. Wang, Z. M. Niu, Y. F. Niu, and B. Sun, Phys. Rev. C **90**, 014303 (2014)
[44] Z. M. Niu, B. H. Sun, H. Z. Liang, Y. F. Niu, and J. Y. Guo, Phys. Rev. C **94**, 054315 (2016)
[45] N. N. Ma, H. F. Zhang, P. Yin, X. J. Bao, and H. F. Zhang, Phys. Rev. C **96**, 024302 (2017)
[46] N. -N. Ma, H. -F. Zhang, X. -J. Bao, H. -F. Zhang, Chin. Phys. C **43**, 044105 (2019)
[47] M. Shi, Z. -M. Niu, H. -Z. Liang, Chin. Phys. C **43**, 074104 (2019)
[48] Z. Niu, H. Liang, B. Sun, Y. Niu, J. Guo, J. Meng, Science Bulletin **63**, 759-764 (2018)
[49] X. J. Bao, H. F. Zhang, B. S. Hu, *et al*., Nucl. Part. Phys. **39**, 095103 (2012)
[50] X. J. Bao, H. F. Zhang, G. Royer, *et al*., Nucl. Phys. A **906**, 1-13 (2013)
[51] H. F. Zhang, Y. J. Wang, J. M. Dong, J. Q. Li, W. Scheid, J. Phys. G, Nucl. Part. Phys. **37**, 085107 (2010)
[52] H. Zhang, W. Zuo, J. Li, G. Royer, Phys. Rev. C **74**, 017304 (2006)
[53] S. Guo, X. Bao, Y. Gao, J. Li, and H. Zhang, Nucl. Phys. A **934**, 110 (2015)
[54] G. Royer, B. Remaud, Nucl. Phys. A **444**, 477 (1985)
[55] G. Royer, J. Phys. G, Nucl. Part. Phys. **26**, 1149 (2000)
[56] G. Royer, R. Gherghescu, Nucl. Phys. A **699**, 479 (2002)
[57] J. Blocki, J. Randrup, W. Swiatecki, C. Tsang, Ann. Phys. **105**, 427 (1977)
[58] J. Dong, W. Zuo, J. Gu, Y. Wang, and B. Peng, Phys. Rev. C **81**, 064309 (2010)
[59] H. F. Zhang, G. Royer, Phys. Rev. C **77**, 054318 (2008)
[60] H. F. Zhang, G. Royer, Y. J. Wang, J. M. Dong, W. Zuo, and J. Q. Li, Phys. Rev. C **80**, 057301 (2009)
[61] O. Nagib, Phys. Rev. C **101**, 014610 (2020)
[62] P. Möller and J. R. Nix, J. Phys. G: Nucl. Part. Phys. **20**, 1681 (1994)
[63] J. J. Li, W. H. Long, Jérôme Margueronc, Nguyen Van Giaib, Phys. Lett. B **732**, 169-173 (2014)
[64] N. Wang, M. Liu, X. Wu, and J. Meng, Phys. Lett. B **734**, 215 (2014)
[65] P. Möller, A. J. Sierka, T. Ichikawa, and H. Sagawa, At. Data Nucl. Data Tables **109**, 1 (2016)